Journal of Organometallic Chemistry, 333 (1987) 403–414
Elsevier Sequoia S.A., Lausanne – Printed in The Netherlands

Asymmetrically bonded π-ligands

II *. Hinging towards metal of substituted allyls: synthesis of three 1-*syn*-$EtOOCC_3H_4$ complexes, and the molecular structure of $[(\eta\text{-}1\text{-}EtOOCC_3H_4)Pd(tmeda)]BF_4$ (tmeda = *N*,*N*,*N*′,*N*′-tetramethylethylenediamine) at 185 K and of $[(\eta\text{-}1\text{-}EtOOCC_3H_4)PdCl]_2$ at 291 K

David P. Grant, Nicholas W. Murrall and Alan J. Welch*
Department of Chemistry, University of Edinburgh, Edinburgh EH9 3JJ (Great Britain)

(Received April 1st, 1987)

Abstract

The 4-, 5- and 6-coordinate complexes $[(\eta\text{-}1\text{-}EtOOCC_3H_4)Pd(tmeda)]BF_4$, $[(\eta\text{-}1\text{-}EtOOCC_3H_4)Pd(\eta\text{-}C_5H_5)]$ and $[(\eta\text{-}1\text{-}EtOOCC_3H_4)RuCl(\eta\text{-}C_6H_6)]$ have been prepared and characterised, and a crystallographic study of the first undertaken. Crystals are triclinic, *Pbar*1, with two ion pairs in a cell of dimensions *a* 7.3076(23), *b* 8.0643(23), *c* 15.632(4) Å, α 89.255(22), β 78.834(22) and γ 76.812(20)° at 185 K. Using 4429 observed data the structure has been refined to $R = 0.0452$, and reveals asymmetry in the Pd–allyl bonding such that the substituted carbon atom is nearer to the metal, Pd–C(1) 2.124(4) Å, than is the unsubstituted allyl terminus, Pd–C(3) 2.131(4) Å. To emphasize the significance of this unusual result the structure of the dimeric precursor $[(\eta\text{-}1\text{-}EtOOCC_3H_4)PdCl]_2$ has been determined. At 291 K one molecule of the dimer crystallises in space group *Pbar*1 in a cell of dimensions *a* 4.9800(18), *b* 6.174(3), *c* 14.080(3) Å, α 86.25(3), β 80.84(3) and γ 89.44(4)° (C_i symmetry imposed). The model has been refined to $R = 0.0499$ for 2239 observed data. In the dimer Pd–C(1) is 2.100(7), Pd–C(3) 2.131(8) Å.

Introduction

In the first paper of this series [1] we outlined the necessary requirements for a systematic study of asymmetrically bonded π-ligands, and reported three crystal

---

* For part I see ref. 1.

structures of (η-1-PhC_3H_4) complexes in which the substituted allylic carbon atom was significantly further from the metal (hinged away) than was the other terminal carbon. From an analysis of the contacts within and between molecules we concluded, certainly for [(η-C_5H_5)Pd(η-1-PhC_3H_4)] and probably for [(η-1-PhC_3H_4)Pd(tmeda)]BF_4, that the asymmetric metal–allyl bonding was electronically induced and not simply a consequence of the bulk of the phenyl substituent.

With the implication that the electronic properties of the substituents terminal to the allyl ligand are in some way responsible for its asymmetric coordination we have attempted to extend our studies to complexes with allyl ligands containing electronically diverse substituents. Herein we describe the syntheses of three ethoxycarbonylallyl complexes, an accurate, low-temperature structural study of [(η-1-EtOOC-C_3H_4)Pd(tmeda)]BF_4 and the room temperature molecular structure of the known dimeric species [(η-1-$EtOOCC_3H_4$)PdCl]$_2$.

Experimental

Syntheses

Schlenk tube techniques were used throughout. The solvents were thoroughly dried and distilled under nitrogen, and degassed before use. The complexes [(η-1-$EtOOCC_3H_4$)PdCl]$_2$ [2] (**1**) and [(η-C_6H_6)$RuCl_2$]$_2$ [3] were prepared by literature methods. ^1H NMR spectra were run on Bruker WP80SY and WP200SY spectrometers, chemical shifts being referenced with respect to those of residual solvent protons known relative to $SiMe_4$, positive shifts to high frequency. IR spectra were recorded on a Perkin–Elmer 598 spectrophotometer, either as a neat liquid or as KBr discs, and melting points, where given, were measured in sealed, evacuated tubes on a Kofler hot stage microscope. C, H, and N microanalyses were determined by the departmental service.

Synthesis of [(η-1-$EtOOCC_3H_4$)Pd(tmeda)]BF_4 (2)

In the procedure described by Schrock and Osborn [4], solid $AgBF_4$ (0.19 g, 1 mmol) was added to a solution of **1** (0.255 g, 0.5 mmol) in CH_2Cl_2 (10 ml), and after ca. 5 min stirring at room temperature tmeda (1.5 ml, 1 mmol) was added. After ca. 1 min the mixture was filtered and the residue of AgCl washed with CH_2Cl_2 (2 × 5 ml). Addition of Et_2O (ca. 100 ml) to the combined filtrate and washings gives [(η-1-$EtOOCC_3H_4$)Pd(tmeda)]BF_4 (**2**) as a white solid. This was recrystallised from Me_2CO/Et_2O (1/3 solvent diffusion at −30 °C) to give diffraction quality crystals; yield 0.35 g, 83%; (Found: C, 34.1; H, 6.1; N, 6.8. $C_{12}H_{25}BF_4N_2Pd$ calc.: C, 34.1; H, 6.0; N, 6.6%); m.p. 124–126 °C; ν_{max} (KBr disc) at 2985, 2900, 1704, 1600, 1510, 1465, 1365, 1313, 1280, 1258, 1155, 1040br, 955, 865, 805 and 770 cm^{-1}. ^1H NMR spectrum [$(CD_3)_2CO$, 298 K]: δ 1.31(t, 7.1 Hz, 3H, CH_3CH_2, 2.66(s, 3H, MeN), 2.92(s, 3H, MeN), 2.9–3.2(m, 4H, $-CH_2-CH_2-$), 3.06(s, 3H, MeN), 3.12(s, 3H, MeN), 3.70(d, 13.3 Hz, 1H, H3a), 3.72(d, 10.3 Hz, 1H, H1a), 4.25(q, 7.1 Hz, 2H, CH_2CH_3), 4.27(d, 7.5 Hz, 1H, H3s) and 6.23(d of d of d, 13.3, 10.3, 7.5 Hz, 1H, H2s) ppm.

Synthesis of [(η-1-$EtOOCC_3H_4$)Pd(η-C_5H_5)] (3)

In an established procedure [5], a thf solution of Na[C_5H_5] (5.0 ml, 0.2 *M*) was added to a solution of **1** (0.25 g, 0.5 mmol) in thf. After 10 min stirring the solution was concentrated to ca. 5 ml and the residue distilled (50 ° C, 0.1 Torr) on to a cold finger (-78 ° C) to afford [(η-1-$EtOOCC_3H_4$)Pd(η-C_5H_5)] (**3**) as a deep red-purple viscous liquid; yield 0.15 g, 53%; ν_{max} (neat) at 3068, 3043, 2986, 2925, 2900, 2867, 1710, 1638sh, 1613, 1477, 1463, 1441, 1388, 1365, 1340, 1306, 1265, 1252, 1217, 1183, 1156, 1096, 1046, 1014, 982, 917, 864, 833, 771 and 735 cm^{-1}. ^1H NMR spectrum ($CDCl_3$, 298 K): δ 1.26(t, 7.1 Hz, 3H, C$H_3$$CH_2$), 2.49(d of d, 11.4, 0.9 Hz, 1H, H3a), 3.17(d, 9.3 Hz, 1H, H1a), 3.74(d, 6.5 Hz, 1H, H3s), 4.15(q, 7.1 Hz, 2H, C$H_2$$CH_3$), 5.73(2, 5H, C_5H_5) and 5.79(d of d of d, 11.4, 9.3, 6.5 Hz, 1H, H2s) ppm.

Synthesis of [(σ-1-$EtOOCC_3H_4$)HgCl] (4)

The procedure described by Nesmeyanov et al. [6] was used. A solution of **1** (0.51 g, 1 mmol) in benzene (10 ml) was stirred vigorously with metallic mercury (10 g) for 1 h, after which the yellow colour had faded. The solution was decanted off and the mercury washed with benzene (2 × 5 ml). The combined solution and washings were evaporated to dryness in vacuo to afford the white solid [(σ-1-$EtOOCC_3H_4$)HgCl] (**4**); yield 0.32 g (92%); m.p. 88–90 ° C; ν_{max} (KBr disc) at 2953, 2910, 2850, 1702, 1623, 1467, 1446, 1388, 1363, 1318, 1198 and 1120 cm^{-1}. ^1H NMR spectrum (C_6D_6, 298 K): δ 1.04(t, 7.1 Hz, 3H, C$H_3$$CH_2$), 1.33(d of d plus sat., 9.0, 1.1 Hz, *J*(H–Hg) 142 Hz, 2H, -CH_2-HgCl), 4.08(q, 7.1 Hz, 2H, C$H_2$$CH_3$), 5.48(d of t, 15.3, 1.1 Hz, 1H, EtOOC-C*H*=CH-) and 6.62(d of t, 15.3, 9.0 Hz, 1H, -CH=C*H*-CH_2-) ppm.

Synthesis of [(η-1-$EtOOCC_3H_4$)RuCl(η-C_6H_6)] (5)

A solution of **4** (0.35 g, 1 mmol) in MeOH (10 ml) was added to a suspension of [(η-C_6H_6)$RuCl_2$]$_2$ (0.25 g, 0.5 mmol) in MeOH/H_2O (100 ml, 10/1) and the mixture was stirred for 16 h, as described by Nesmeyanov and Rubezhov [7]. The solution was then filtered and diluted with H_2O (250 ml), and the product was extracted with CH_2Cl_2 (5 × 50 ml). The extracts were dried over $MgSO_4$ then evaporated under reduced pressure. The residue was recrystallised from CH_2Cl_2/n-hexane (1/3, solvent diffusion) to afford orange crystals of [(η-1-$EtOOCC_3H_4$)-RuCl(η-C_6H_6)] (**5**): yield 0.18 g, 55%; (Found: C, 44.2; H, 4.6. $C_{12}H_{15}ClO_2Ru$ calc.: C, 44.0; H, 4.6%); m.p. 210 ° C (dec.); ν_{max} (KBr disc) at 3040, 2945, 2905, 2853, 1675, 1487, 1433, 1364, 1300, 1215, 1145, 1047, 916, 868, 849 and 805 cm^{-1}. ^1H NMR spectrum [$(CD_3)_2CO$, 298 K]: δ 1.25(t, 7 Hz, 3H, C$H_3$$CH_2$), 2.32(d, 12 Hz, 1H, H3a), 2.37(d, 8 Hz, 1H, H3s), 2.87(d, 10 Hz, 1H, H1a), 4.21(q, 7 Hz, 2H, C$H_2$$CH_3$), 5.12(d of d of d, 12, 10, 8 Hz, 1H, H2s) and 5.60(s, 6H, C_6H_6) ppm.

Crystallographic studies

Complex **3** is a liquid at ambient temperature, and appears to freeze between -20 and -30 ° C at 1 atm, since solid rapidly melts on removal from a freezer kept at -30 ° C. Although techniques for in situ crystal growth and low temperature X-ray diffraction are well developed at Edinburgh [8], we have not yet attempted to study **3** by this method.

Crystals of **5** showed very poor optical properties under a polarising microscope, and did not yield discrete spots on a Weissenberg camera. No better crystals could be grown by numerous recrystallisations from a variety of solvents or solvent mixtures.

In contrast, **1** and **2** form as well-developed single crystals, the former being

Table 1

Crystallographic data for **1** and **2**

	1	**2**
Formula	$C_{12}H_{18}Cl_2OPd_2$	$C_{12}H_{25}BF_4N_2Pd$
Mol.wt.	510.0	422.5
Crystal size (mm)	0.4×0.2×0.2	0.4×0.3×0.3
System	triclinic	triclinic
Space group	$P\bar{1}$	$P\bar{1}$
Temperature (K)	291 ± 1	185 ± 1
a (Å)	4.9800(18)	7.3076(23)
b (Å)	6.174(3)	8.0643(23)
c (Å)	14.080(3)	15.632(4)
α (°)	86.25(3)	89.255(22)
β (°)	80.84(3)	78.834(22)
γ (°)	89.44(4)	76.812(20)
U (Å^3)	424.6	879.4
Z	1	2
D_x (g cm^{-3})	1.994	1.595
$F(000)$	248	428
μ(Mo-$K_{\bar{\alpha}}$) (cm^{-1})	24.16	10.85
θ range for setting angles (°)	14.0–20.0	12.0–13.0
θ range for data (°)	1.0–30.0	1.0–30.0
Scan speed range (° min^{-1})	1.03–3.30	1.03–5.49
Reflections measured	$+h \pm k \pm l$	$+h \pm k \pm l$
Total data	2607	5502
Unique data	2440	5110
R merge	0.0166	0.0162
X-ray exposure (h)	55	133
Data with $F > 2.0\sigma(F)$	2239	4429
g	0.00029	0.00190
U [a] allyl-H (Å^2)	0.08	0.06
U methylene-H (Å^2)	–	0.06
U methyl-H (Å^2)	–	0.06
R [b]	0.0499	0.0452
R_w [c]	0.0582	0.0616
S [d]	1.7051	0.9894
No. variables	124	226
Max. residual peak (eÅ^{-3})	1.55	1.31
Min. residual trough (eÅ^{-3})	−1.68	−0.91

[a] The isotropic temperature factor defined as $\exp[-8\pi^2U(\sin^2\theta)/\lambda^2]$. [b] $R = [\Sigma|F_o - |F_c||/\Sigma F_o]$. [c] $R_w = [\Sigma w|F_o - |F_c||^2/\Sigma wF_o^2]^{1/2}$. [d] S is the e.s.d. of an observation of unit weight.

obtained by solvent diffusion (CH_2Cl_2/n-hexane, 1/3, −30 °C). A single crystal of **1** was glued to a thin glass fibre, whilst a specimen of **2** was sealed under N_2 in a Lindemann capillary with low temperature epoxy-resin adhesive. Unit-cell dimensions were determined on an Enraf–Nonius CAD4 diffractometer by the least-squares refinement of 25 centred angles measured using graphite-monochromated Mo-K_α radiation, λ 0.71069 Å. Table 1 lists crystal parameters, details of intensity data collection, and information relating to structure solution and refinement.

In both cases data were collected by $\omega:2\theta$ scans in 96 steps (ω scan width $0.8 + 0.35 \tan\theta$) at variable speeds dependent upon an initial prescan. Constant remonitoring of check reflections ultimately revealed no significant movement or decay. Data from **2** were not corrected for X-ray absorption; those from **1** were corrected empirically [9] after isotropic convergence. After merging equivalent reflections, only those with $F > 2.0\sigma(F)$ were retained for structure solution and refinement. In both cases the centrosymmetric space group *Pbar*1 was confirmed by successful refinement [for **1** the disordered model in *Pbar*1 is preferred [10] to an ordered one in *P*1].

The structures were solved by Patterson (Pd, Cl) and iterative full-matrix least-squares refinement (on F) and ΔF syntheses. Data were weighted according to $w^{-1} = [\sigma^2(F) + gF^2]$. Allylic H atoms were located from ΔF maps and positionally refined, freely for **2** but with a common C–H distance (0.98(4) Å at convergence) for **1**. For **2** all other H atoms were set in idealised positions, riding on their respective C atom with C–H 1.08 Å. For **1** the EtOO fragment is equally disordered over two sites. Like bond distances were restrained to the same values under refinement, converging at 1.195(15) Å (C=O), 1.348(13) Å (C–OEt), 1.469(17) Å (O–C_2H_5) and 1.40(3) Å (C–C).

Refinements were cycled to convergence, and final ΔF maps were computed with all data. Programs and packages used were SHELX76 [11], XANADU [12], CALC [13] and XRAY76 [14] for solution, refinement and molecular geometry calculations, and ORTEP-II [15] and SCHAKAL [16] for plotting, all implemented on the Edinburgh Regional Computer Centre ICL 2972 computer. For Pd, coefficients for an analytical form of the scattering curve were taken from ref. 17, whilst inlaid [11] neutral atom scattering factors were used for all other atoms. Refined positional parameters of **1** and **2** are listed in Table 2 and Table 3, respectively. Tables of thermal parameters, least-squares planes (for **2**), significant non-bonded contacts (for **2**), and lists of observed and calculated structure factors are available from the authors.

Table 2

Fractional coordinates of refined atoms in **1**

Atom	*x*	*y*	*z*
Pd	0.22858(7)	0.13133(5)	0.41209(3)
Cl	0.0527(4)	0.1853(3)	0.57711(12)
C(1)	0.4339(15)	0.1244(12)	0.2700(5)
C(2)	0.4216(15)	0.3395(11)	0.2985(5)
C(3)	0.5260(15)	0.3836(12)	0.3809(6)
C(4)	0.2652(18)	0.0597(13)	0.1984(5)
O(1)	0.133(7)	0.178(4)	0.154(3)
O(2)	0.357(6)	−0.135(3)	0.1695(21)
C(5)	0.226(7)	−0.226(5)	0.095(3)
C(6)	−0.041(7)	−0.291(5)	0.1321(20)
O(1′)	0.091(5)	0.179(4)	0.176(3)
O(2′)	0.276(6)	−0.1571(19)	0.1873(17)
C(5′)	0.112(5)	−0.238(3)	0.1190(15)
C(6′)	0.269(6)	−0.288(6)	0.0314(23)
H(12)	0.600(11)	0.044(10)	0.279(5)
H(31)	0.478(15)	0.535(7)	0.394(5)
H(32)	0.673(12)	0.284(9)	0.393(5)
H(21)	0.312(13)	0.457(9)	0.274(5)

Table 3

Fractional coordinates of atoms in **2**

Atom	x	y	z
Pd	0.12041(4)	0.16249(3)	0.76001(2)
C(1)	0.1063(7)	0.0791(5)	0.8900(3)
C(2)	−0.0598(7)	0.0624(6)	0.8611(3)
C(3)	−0.0346(8)	−0.0328(6)	0.7847(4)
C(4)	0.0899(6)	0.1998(5)	0.9635(3)
C(5)	0.2658(7)	0.3038(7)	1.0542(3)
C(6)	0.4672(10)	0.2857(16)	1.0581(6)
O(1)	−0.0562(5)	0.2956(5)	0.99905(23)
O(2)	0.2593(4)	0.1860(4)	0.98473(20)
N(1)	0.1267(5)	0.1923(5)	0.62425(22)
N(2)	0.3049(5)	0.3347(4)	0.74399(21)
C(7)	0.2158(13)	0.3399(11)	0.6010(4)
C(8)	0.3684(10)	0.3416(9)	0.6476(3)
C(9)	0.2307(9)	0.0343(9)	0.5771(4)
C(10)	−0.0643(8)	0.2412(7)	0.6009(3)
C(11)	0.4805(6)	0.2730(7)	0.7781(4)
C(12)	0.2060(7)	0.5000(5)	0.7875(4)
B	0.6629(10)	0.7441(7)	0.6744(4)
F(1)	0.5947(6)	0.6634(5)	0.61524(23)
F(2)	0.7585(8)	0.6332(6)	0.7236(3)
F(3)	0.7548(17)	0.8514(14)	0.6347(4)
F(4)	0.5153(12)	0.8403(10)	0.7300(5)
H(12)	0.234(9)	−0.023(8)	0.885(4)
H(21)	−0.211(9)	0.163(8)	0.881(4)
H(31)	−0.126(9)	−0.029(8)	0.749(4)
H(32)	0.133(9)	−0.144(8)	0.755(4)
H(51)	0.1882	0.2716	1.1158
H(52)	0.2035	0.4331	1.0394
H(61)	0.4517	0.3912	1.1028
H(62)	0.4959	0.3270	0.9918
H(63)	0.5847	0.1838	1.0684
H(71)	0.1069	0.4563	0.6172
H(72)	0.2735	0.3326	0.5318
H(81)	0.4846	0.2325	0.6257
H(82)	0.4182	0.4570	0.6332
H(91)	0.3696	−0.0311	0.5887
H(92)	0.2399	0.0566	0.5083
H(93)	0.1286	−0.0431	0.5983
H(101)	−0.1237	0.1309	0.6157
H(102)	−0.0530	0.2656	0.5322
H(103)	−0.1567	0.3505	0.6385
H(111)	0.4135	0.2640	0.8454
H(112)	0.5699	0.3638	0.7737
H(113)	0.5674	0.1497	0.7536
H(121)	0.0674	0.5437	0.7700
H(122)	0.2906	0.5932	0.7692
H(123)	0.1878	0.4830	0.8570

Results and discussion

Bridge cleavage of $[(\eta\text{-1-EtOOCC}_3H_4)PdCl]_2$ (**1**) with $AgBF_4$/tmeda or with $Na[C_5H_5]$ has afforded the new complexes $[(\eta\text{-1-EtOOCC}_3H_4)Pd(tmeda)]BF_4$ (**2**) and [(η-1-EtOOCC$_3$H$_4$)Pd(η-C$_5$H$_5$)] (**3**) respectively, in moderate yields. The dimer is also cleaved by mercury to afford the σ-bonded organomercury complex [(σ-1-EtOOCC$_3$H$_4$)HgCl] (**4**), which acts as an efficient allylating agent in the synthesis of [(η-1-EtOOCC$_3$H$_4$)RuCl(η-C$_6$H$_6$)] (**5**) by bridge cleavage of [(η-C$_6$H$_6$)RuCl$_2$]$_2$.

Satisfactory elemental analyses were recorded for the solid π-bonded complexes **2** and **5**, and all new species show a characteristic C=O stretch in the IR spectrum at 1700 ± 25 cm^{-1}. ^{1}H NMR spectra of complexes **2**, **3** and **5**, with the allylic protons labelled as in the line diagram (**6**), are fully consistent with the presence of a

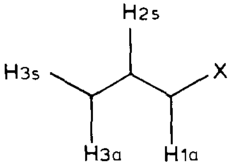

(**6**)

1-*syn*-ethoxycarbonylallyl ligand. In the ^{1}H NMR spectrum of **4** satellites due to ^{199}Hg are clearly evident on the methylene signal, and the spectrum compares favourably with those of analogous σ-bonded allyl species [18].

Complexes **2**, **3** and **5** satisfy the requirement [1] that an asymmetrically substituted allyl is bound to an otherwise symmetric metal fragment. Of these it has, unfortunately, been possible to study only **2** by a diffraction experiment, and, in keeping with the need for as accurate study as possible, this has been performed carefully, at low temperature, to a relatively high value of (sin θ)/λ.

The dimer **1** has been known for a considerable time [2] but has not before been studied crystallographically. Although, strictly, the molecular fragment opposite each allyl ligand is not symmetric, (since it contains a deliberately asymmetric allyl) that portion of the molecule which constitutes the immediate metal coordination sphere is. Therefore we have also investigated **1** by a diffraction experiment. It has proved necessary to perform this at room temperature since cooling **1** to below ca. 10 °C appears to cause a phase change which is accompanied by a severe reduction in crystal quality.

A perspective view of a single cation of **2** is shown in Fig. 1, together with the atomic numbering scheme adopted. For comparative purposes numbering within the coordination sphere of the metal is the same as that [1] in the phenylallyl analogue [(η-1-PhC$_3$H$_4$)Pd(tmeda)]BF$_4$ (**7**). Interatomic distances and interbond angles are given in Table 4.

A unit cell packing diagram is available from the authors. Anions and cations are reasonably well separated in the crystal, there being only four F — — — H contacts of possible importance, 2.31–2.45 Å, all involving H atoms of the tmeda ligand.

The $\overline{\text{PdNCCN}}$ cycle in **2** adopts the alternative skew conformation, relative to the substituted allyl function, than it does in **7**, with the CH$_2$–CH$_2$ bond lying roughly parallel to C(1)–C(2). In **2** the disposition of the methylene carbon atoms with respect to the PdN$_2$ plane is quite regular, C(7) lying 0.30 Å to one side and C(8) 0.33 Å to the other, but this is not the case in **7** (deviations of 0.51 and 0.18 Å). The more symmetric arrangement in **2** evidently allows for a somewhat more compact tmeda ligand, since the N–Pd–N angles in the two complexes are identical to within

Table 4

Interatomic distances (Å) and interbond angles (°) for **2**

Pd–C(1)	2.124(4)	N(1)–C(7)	1.491(9)
Pd–C(2)	2.128(4)	N(1)–C(9)	1.452(8)
Pd–C(3)	2.131(4)	N(1)–C(10)	1.476(7)
Pd–N(1)	2.125(3)	N(2)–C(8)	1.493(7)
Pd–N(2)	2.127(3)	N(2)–C(11)	1.465(6)
C(1)–C(2)	1.408(7)	N(2)–C(12)	1.468(6)
C(2)–C(3)	1.388(7)	C(7)–C(8)	1.448(10)
C(1)–C(4)	1.484(6)	B–F(1)	1.366(7)
C(4)–O(1)	1.204(6)	B–F(2)	1.336(8)
C(4)–O(2)	1.323(5)	B–F(3)	1.294(12)
C(5)–C(6)	1.458(11)	B–F(4)	1.339(10)
C(5)–O(2)	1.467(6)		
		C(3)–H(32)	1.35(5)
C(1)–H(12)	1.08(6)	C(3)–H(31)	0.94(6)
C(2)–H(21)	1.20(6)	C(1)–H(12)	1.35(6)
C(1)–Pd–C(2)	38.69(18)	C(4)–O(2)–C(5)	115.8(4)
C(1)–Pd–C(3)	68.32(19)	Pd–N(1)–C(7)	105.2(4)
C(1)–Pd–N(1)	167.54(16)	Pd–N(1)–C(9)	109.6(3)
C(1)–Pd–N(2)	106.03(15)	Pd–N(1)–C(10)	114.3(3)
C(2)–Pd–C(3)	38.03(20)	C(7)–N(1)–C(9)	114.3(5)
C(2)–Pd–N(1)	133.39(17)	C(7)–N(1)–C(10)	105.3(5)
C(2)–Pd–N(2)	139.65(16)	C(9)–N(1)–C(10)	108.3(4)
C(3)–Pd–N(1)	100.35(18)	Pd–N(2)–C(8)	104.6(3)
C(3)–Pd–N(2)	171.85(18)	Pd–N(2)–C(11)	113.6(3)
N(1)–Pd–N(2)	84.67(14)	Pd–N(2)–C(12)	110.8(3)
Pd–C(1)–C(2)	70.8(3)	C(8)–N(2)–C(11)	105.6(4)
Pd–C(1)–C(4)	121.2(3)	C(8)–N(2)–C(12)	114.4(4)
C(2)–C(1)–C(4)	119.7(4)	C(11)–N(2)–C(12)	107.8(4)
Pd–C(2)–C(1)	70.5(3)	N(1)–C(7)–C(8)	112.0(6)
Pd–C(2)–C(3)	71.1(3)	N(2)–C(8)–C(7)	112.4(6)
C(1)–C(2)–C(3)	117.4(4)	F(1)–B–F(2)	111.7(5)
Pd–C(3)–C(2)	70.9(3)	F(1)–B–F(3)	109.4(6)
C(1)–C(4)–O(1)	125.2(4)	F(1)–B–F(4)	109.4(6)
C(1)–C(4)–O(2)	110.0(4)	F(2)–B–F(3)	115.7(7)
O(1)–C(4)–O(2)	124.9(4)	F(2)–B–F(4)	105.5(6)
C(6)–C(5)–O(2)	106.9(5)	F(3)–B–F(4)	104.7(7)
Pd–C(1)–H(12)	103.5(33)	C(5)–C(6)–H(63)	136.6(10)
H(12)–C(1)–C(2)	123.8(33)	N(1)–C(9)–H(91)	121.0(7)
H(12)–C(1)–C(4)	110.7(33)	N(1)–C(9)–H(92)	107.6(6)
Pd–C(2)–H(21)	109.3(30)	N(1)–C(9)–H(93)	99.1(6)
C(1)–C(2)–H(21)	122.7(30)	N(1)–C(10)–H(101)	104.1(5)
H(21)–C(2)–C(3)	115.8(30)	N(1)–C(10)–H(102)	111.2(5)
Pd–C(3)–H(31)	114.1(38)	N(1)–C(10)–H(103)	113.0(6)
Pd–C(3)–H(32)	86.9(25)	N(2)–C(11)–H(111)	97.5(5)
C(2)–C(3)–H(31)	126.3(39)	N(2)–C(11)–H(112)	113.6(5)
C(2)–C(3)–H(32)	120.3(26)	N(2)–C(11)–H(113)	116.6(5)
H(31)–C(3)–H(32)	113.4(46)	N(2)–C(12)–H(121)	110.4(5)
C(5)–C(6)–H(61)	98.7(9)	N(2)–C(12)–H(122)	110.3(5)
C(5)–C(6)–H(62)	90.4(9)	N(2)–C(12)–H(123)	107.7(5)

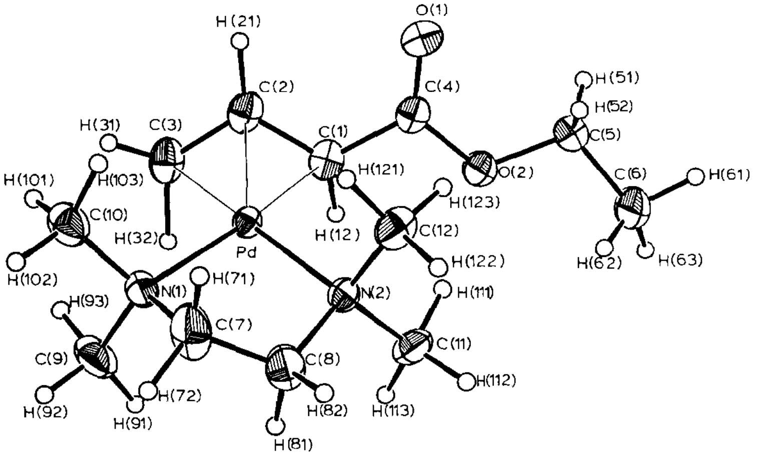

Fig. 1. Perspective view of the cation of [(η-1-EtOOCC$_3$H$_4$)Pd(tmeda)]BF$_4$ (**2**).

1 e.s.d. yet the Pd–N distances in **2**, internally equivalent, are ca. 0.01–0.02 Å, shorter than those in **7**.

Parameters [β, τ, δ_1, h_i ($i = 1$–3)] that describe the stereochemistry of a π-bonded allyl ligand have been described by others [19,20] and used by us in the previous paper in this series [1]. In **2** herein, τ is 117.6° [identical to that in **7**] and δ_1 is 118.3° [120.5° in **7**]. The better agreement between τ and δ_1 for **2** cf. **7** suggests that in **2** the allyl is bound more symmetrically across the metal coordination plane, and this is confirmed by the similarity of h_1 and h_3, 0.2315 and 0.2370 Å respectively (for completeness h_2 is -0.4056 Å). These values in turn suggest little "rotation" of the allyl about the Pd–allyl axis, and consistent with this are the observations that the C–C allyl bond lengths in **2** are more similar, 1.388(7) and 1.408(7) Å, than those in **7**, and that the C(1)–C(2)–C(3) angle is less close to 120°.

The C(3)–H(32) bond appears to be abnormally long, 1.35(5) Å, and we do not understand why. However, the elevation angles of the H atoms relative to the C$_3$ plane are as expected, with the *syn* H's bent towards Pd, by 19.9° [H(21)] and 15.0° [H(31)], and the *anti* H's bent away, by 31.2° [H(12)] and 16.7° [H(32)].

In **2** the EtOOC substituent is oriented such that O(1) is *syn* to C(2) and C(5)–C(6) is roughly parallel to C(4)–O(2). There is a slight twist about the C(1)–C(4) bond (12.0°) such that O(1) is tilted towards, and O(2) away from, the palladium atom. There are no close interligand contacts within the cation, but O(1) and H(52) are involved in a doubly H-bonded cycle with each other across the inversion centre at (0 1/2 1) [O – – – H 2.333(6) Å, C=O – – – H 129.9(3)°, O – – – H–C 175.8(6)°], and it is possible that this is at least partially responsible for the –C(1)–C(4)– torsion.

The central allyl carbon, C(2), is not nearer to the metal atom than the terminal carbons. This is reasonably unusual [19,20]; in other complexes where it has also been observed, e.g. [{Me$_2$Ga(N$_2$C$_5$H$_7$)(OCH$_2$CH$_2$NH$_2$)}Mo(CO)$_2$(η-2-MeC$_3$H$_4$)] [21], [(η-C$_9$H$_7$)Mo(CO)$_2$(η-2-MeC$_3$H$_4$)] [22] and [(η-C$_5$H$_5$)Mo(RCN)$_2${η-RCN · C(CH$_2$Bu^t) · CNR}] (R = 2,6-Me$_2$C$_6$H$_3$) [23] there is generally a substituent on C(2) which acts in a repulsive sense with other ligands. In **2** Pd–C(2) is the intermediate Pd–C distance.

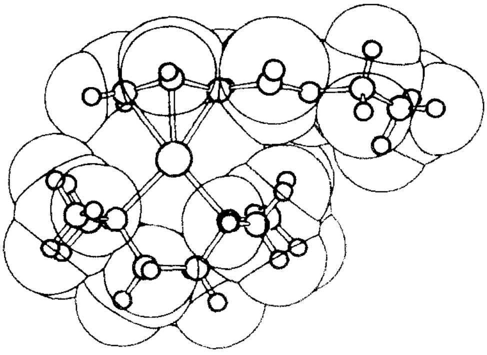

Fig. 2. Space filling diagram of the cation of **2**.

Of considerable interest in a study of asymmetrically bonded π ligands is the observation that in **2** the carbon carrying the EtOOC substituent, C(1), is actually closer to the metal atom, 2.124(3) Å, than is the other C terminus, C(3), 2.131(4) Å, resulting in an obtuse β angle, 90.3°. We fully appreciate that the difference between the Pd–C(1,3) lengths is not strictly statistically significant. Nevertheless, we believe that this hinging towards metal of the substituted allyl is relevant for the following reasons:

(i) Everything else being equal one might expect that intramolecular interligand contacts would cause hinging in the opposite direction. Although Fig. 2, a space filling representation of the cation of **2**, shows efficient packing of tmeda and $EtOOCC_3H_4$ ligands around the metal, calculations reveal no such contacts within

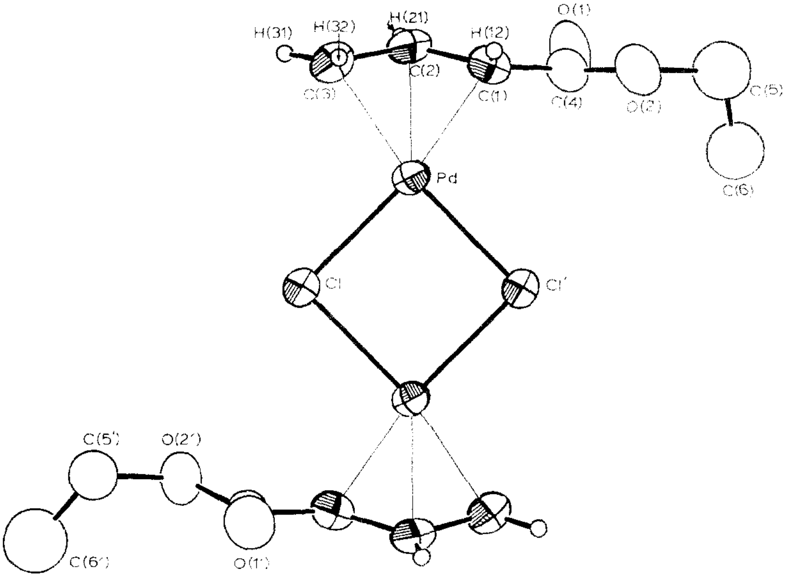

Fig. 3. The dimer $[(\eta\text{-}1\text{-}EtOOCC_3H_4)PdCl]_2$ (**1**). The EtOO fragments are disordered, and for clarity each of the two different sequences is shown on different halves of the molecule.

Table 5

Bond lengths (Å) and interbond angles (°) in **1**

Pd–Cl	2.3922(18)	Pd–C(3)	2.131(8)
Pd–Cl′	2.3917(18)	C(1)–C(2)	1.405(10)
Pd–C(1)	2.100(7)	C(1)–C(4)	1.486(11)
Pd–C(2)	2.095(7)	C(2)–C(3)	1.388(11)
Cl–Pd–Cl′	88.85(6)	C(1)–C(2)–C(3)	118.4(7)
Cl–Pd–C(1)	170.02(20)	C(1)–C(2)–H(21)	125.9(38)
Cl–Pd–C(2)	132.79(20)	C(3)–C(2)–H(21)	114.4(38)
Cl–Pd–C(3)	101.05(21)	Pd–C(3)–C(2)	69.4(4)
Cl′–Pd–C(1)	100.88(20)	Pd–C(3)–H(31)	121.0(40)
Cl′–Pd–C(2)	134.64(20)	Pd–C(3)–H(32)	92.5(39)
Cl′–Pd–C(3)	169.09(21)	C(2)–C(3)–H(31)	106.5(40)
C(1)–Pd–C(2)	39.1(3)	C(2)–C(3)–H(32)	112.5(39)
C(1)–Pd–C(3)	69.1(3)	H(31)–C(3)–H(32)	135.7(55)
C(2)–Pd–C(3)	38.3(3)	C(1)–C(4)–O(1)	126.4(18)
Pd–C(1)–C(2)	70.2(4)	C(1)–C(4)–O(2)	106.9(13)
Pd–C(1)–C(4)	115.2(5)	C(1)–C(4)–O(1′)	120.3(16)
Pd–C(1)–H(12)	102.3(38)	C(1)–C(4)–O(2′)	112.1(11)
C(2)–C(1)–C(4)	119.6(7)	O(1)–C(4)–O(2)	123.5(21)
C(2)–C(1)–H(12)	115.6(38)	O(1′)–C(4)–O(2′)	124.8(19)
C(4)–C(1)–H(12)	120.6(38)	C(4)–O(2)–C(5)	116.0(23)
Pd–C(2)–C(1)	70.6(4)	O(2)–C(5)–C(6)	110.5(27)
Pd–C(2)–C(3)	72.2(4)	C(4)–O(2′)–C(5′)	116.2(18)
Pd–C(2)–H(21)	117.1(38)	O(2′)–C(5′)–C(6′)	112.9(22)

the Van der Waals sums.

(ii) Apart from F — — — H(tmeda), the only apparent intermolecular contacts are those of the H-bonded cycle involving O(1) — — — H(52), and H(63) to H(12) at $(1 - x, y, 2 - z)$, 1.87(6) Å. The direction of the O — — — H bond suggests that, if anything, these forces would lengthen Pd–C(1). The importance of the H — — — H contact is in some doubt since it is possibly only an artefact of an ill-defined $C(6)H_3$ function, treated as a rigid group in the X-ray study (H–C–H angles 109.47°), but refining to rather dubious C(5)–C(6)–H angles, 98.7, 90.4 and 136.6° to H(61), H(62) and H(63), respectively.

(iii) The structural determination of the centrosymmetric dimer **1**, Fig. 3, reveals hinging in the same sense. Although, as we have already pointed out, **1** is not a strictly valid example of a species with a symmetric non-allyl ligand set, asymmetry in the metal–allyl bonding is relevant to the structure of **2** because; (a) the two *trans* bonded ligands, Cl and Cl′, are equally bound to Pd; (b) the allylic conformation is the same as, and dimensions within the allyl fragment are very similar to, those in **2**; (c) there are no close intermolecular contacts in the crystal of **1**. Molecular parameters for the dimer are listed in Table 5. Pd–C(1) is shorter than Pd–C(3) by 0.031(11) Å, i.e. $\Delta/\sigma > 2.9$.

Thus, the implication that arises from the observed hinging of C(1) towards the metal atom in **1** and **2** is that the distortion is electronically induced. This phenomenon, together with the complimentary one of hinging of 1-PhC_3H_4 ligands in the opposite sense [1], will be the subject of a theoretical study in the third contribution in this series [24].

Acknowledgements

We are grateful to the Chemistry Department of Edinburgh University for a research studentship (N.W.M.), and to Johnson Matthey plc for a loan of palladium chloride.

References

1 Part I. N.W. Murrall and A.J. Welch, J. Organomet. Chem., 301 (1986) 109.
2 J. Tsuji and S. Imamura, Bull. Chem. Soc. Jap., 40 (1967) 197.
3 R.A. Zelonka and M.C. Baird, Canad. J. Chem., 50 (1972) 3063.
4 R.R. Schrock and J.A. Osborn, J. Am. Chem. Soc., 93 (1971) 3089.
5 S.D. Robinson and B.L. Shaw, J. Chem. Soc., (1963) 4806.
6 A.N. Nesmeyanov, A.Z. Rubezhov, L.A. Leites and S.P. Gubin, J. Organomet. Chem., 12 (1968) 187.
7 A.N. Nesmeyanov and A.Z. Rubezhov, J. Organomet. Chem., 164 (1979) 259.
8 A.J. Blake, S. Cradock, E.A.V. Ebsworth, D.W.H. Rankin and A.J. Welch, J. Chem. Soc., Dalton Trans., (1984) 2029.
9 N.G. Walker and D. Stuart, Acta Crystallogr., Sect. A, 39 (1983) 158.
10 R.E. Marsh, Acta Crystallogr., Sect. B, 42 (1986) 193.
11 G.M. Sheldrick, SHELX76, University Chemical Laboratory, Cambridge, 1976.
12 P. Roberts and G.M. Sheldrick, XANADU, University Chemical Laboratory, Cambridge, 1976.
13 R.O. Gould and P. Taylor, CALC, University of Edinburgh, 1986.
14 J.M. Stewart, P.A. Machin, C.W. Dickinson, H.L. Ammon, H. Heck and H. Flack, Tech. Rep. TR446, Computer Science Centre, University of Maryland, 1976.
15 C.K. Johnson, Rep. ORNL-5138, Oak Ridge National Laboratory, Tennessee, 1976.
16 E. Keller, SCHAKAL, University of Freiburg, 1980.
17 International Tables for X-Ray Crystallography, Kynoch Press, Birmingham, 1974, Vol. 4.
18 A.J. Graham and R.H. Fenn, J. Organomet. Chem., 37 (1972) 137.
19 J.A. Kaduk, A.T. Poulos and J.A. Ibers, J. Organomet. Chem., 127 (1977) 245.
20 C.F. Putnik, J.J. Welter, G.D. Stucky, M.J. D'Aniello Jnr., B.A. Sosinsky, J.F. Kirner and E.L. Muetterties, J. Am. Chem. Soc., 100 (1978) 4107.
21 K.S. Chong, S.J. Rettig, A. Storr and J. Trotter, Canad. J. Chem., 57 (1979) 1335.
22 A.J. Welch, unpublished results.
23 D.S. Gill, P.K. Baker, M. Green, K.E. Paddick, M. Murray and A.J. Welch, J. Chem. Soc., Chem. Commun., (1981) 986.
24 E.J.M. Hamilton, D.P. Grant, N.W. Murrall and A.J. Welch, in preparation.